Available online at www.sciencedirect.com
SCIENCE DIRECT®
Solid State Nuclear Magnetic Resonance 29 (2006) 191–198
Solid State Nuclear Magnetic Resonance
www.elsevier.com/locate/ssnmr

Towards rapid throughput NMR studies of full wine bottles

Daniel N. Sobieski, Gene Mulvihill[1], Joseph S. Broz[2], Matthew P. Augustine*,[1]

Department of Chemistry, One Shields Avenue, University of California, Davis, CA 95616, USA

Received 1 July 2005

Abstract

A rapid throughput method for the quantitation of the oxidation level of intact full bottles of wine based on the $1\bar{3}3\bar{1}$ water suppression pulse sequence is described. The ideal pulse sequence suppresses water in the ^{1}H nuclear magnetic resonance spectrum while uniformly and phase coherently exciting the resonances pertaining to ethyl alcohol at 1.1 ppm and oxidation products at 2.1 ppm. The anticipated results of the pulse sequence based on simulations are tested in small sample and full bottle standards and an application to the detection of wine spoilage in more than century old wine is provided.

Keywords: Water suppression; Wine; Rapid throughput

1. Introduction

It is well known that nuclear magnetic resonance (NMR) spectroscopy is one of if not the most powerful tool available to study the structure of molecules in solids, liquids, and gases with unprecedented resolution [1]. Indeed the phenomenon of NMR is not just limited to the study of chemical compounds where the relationship between peak position, intensity, and structure is exploited [2]. Rather the non-invasive and non-destructive aspects of radio frequency spectroscopy have been used to develop the field of magnetic resonance imaging (MRI) [3,4]. Although in principle much lower resolution in comparison to NMR due to the requirement for switchable inhomogeneous magnetic fields, several MRI applications that endeavor to correlate the structure of molecules in targeted regions inside an object have been pursued. This marriage of NMR and MRI has led to the development of functional MRI [5] and NMR microscopy [6], spectroscopic techniques with applications ranging from rheology [7] to enology [8–11].

The NMR study of wine and associated enological problems is well documented and involves two separate classes of experiments related by the use of standard small sample volumes [12–23]. One approach uses natural abundance deuterium NMR spectroscopy to finger print native wine samples and relies on the geographical dependence of the amount of deuterium in rainfall [12,14–16]. Here the deuterium in rainwater is incorporated into grapes during growth and ultimately parsed into the methylene and methyl groups in ethyl alcohol during fermentation. Specifically, comparison of the ratio of the amount of deuterium in water and the amount of deuterium in the methylene and methyl functionalities in ethyl alcohol for an unknown wine measured from a standard natural abundance deuterium NMR spectrum to data base values is used to identify specific vintages and types of French wine. In a similar vein high field high resolution NMR spectroscopy has been used to finger print wines based on amino acid content [18,19]. The second class of small sample experiments uses standard multi-dimensional liquid state NMR spectroscopy to study the components of wine isolated using chemical separation methods [20–23].

This report also involves the study of native wine samples but with a different focus from the small sample study mentioned above. Specifically, NMR spectroscopy is

*Corresponding author. Fax: +1 530 752 8995.
E-mail address: augustin@chem.ucdavis.edu (M.P. Augustine).
[1]Current address: Wine Scanner, Inc., 355 Madison Avenue, Morristown, NJ 07960, USA.
[2]Current address: TQSM Division, Midwest Research Institute, 518 17th Street 17th Floor, Denver, CO 80202, USA.1

0926-2040/$ - see front matter © 2005 Elsevier Inc. All rights reserved.
doi:10.1016/j.ssnmr.2005.08.014

used to identify spoiled full bottles of wine without opening the bottle and thus devaluing the wine [8,9]. Collectible rare wine spoils according to three dominant mechanisms related to corks. Vinegarization and maderization, or the oxidation of ethyl alcohol into acetic acid and acetaldehyde respectively, is mediated by leaky corks [24–26]. These two spoilage mechanisms affect roughly 5–10% of all collectible wine [27] and involve the reaction of oxygen with ethyl alcohol. Both of these spoilage mechanisms are reasonable targets for full bottle NMR measurements as oxidized wine contains in excess of 1.4 g/L acetic acid and 300 mg/L of acetaldehyde [24–26]. The third dominant spoilage mechanism is cork taint or the production of 2,4,6-trichloroanisole (TCA) by cork mold and again affects roughly 5–10% of all collectible wine [28]. Unfortunately the detection of TCA in full bottles of wine by NMR spectroscopy is not practical as the human pallet is sensitive to ~10 ng/L sub-NMR detection threshold quantities [29].

The original work involving the NMR of full wine bottles [8–11] and the specific study of leaky cork mediated vinegarization and maderization of full wine bottles [8,9] is adequately characterized as an academic curiosity. These studies involved either expensive MRI equipment [10,11] or required the lengthy optimization of frequency selective pulse sequences to minimize the effects of water on full bottle ^{1}H NMR spectra [8,9]. However, careful examination of the high end wine collection market suggests that roughly nine million bottles of collectible red wine are cellared and given that 5–10% of these bottles are oxidized, 450,000–900,000 bottles of spoiled wine [27] could be identified by full bottle NMR spectroscopy. Since the wine auction market routinely resells collectible wines, the full bottle NMR method offers a non-invasive way to insure the serious wine collector or buyer that the auctioned product is pristine or equivalently not spoiled due to leaky cork mediated ethyl alcohol oxidation. This market analysis motivates the need for an inexpensive rapid throughput NMR method capable of studying full wine bottles.

The design of an appropriate instrument to meet the goal of full wine bottle analysis reflects both cost and the acquisition of high-resolution ^{1}H NMR spectra. Here the resonance for water at 4.7 ppm must be suppressed in order to reveal the methyl group resonances for acetic acid or acetaldehyde at 2.1 ppm. In situations where the degree of wine spoilage is necessary, the methyl group proton peak for ethyl alcohol at 1.1 ppm must also be observed as the ratio of the 2.1 to 1.1 ppm integrated peak intensities is the ratio of oxidation products to ethyl alcohol in the full wine bottle. Therefore, the ideal full bottle NMR method requires less than 1 ppm magnetic field inhomogeneity over the wine bottle volume coupled with uniform rf excitation in the 1–2 ppm range with reasonable water suppression. The requirement for adequate field homogeneity is easily met in high $B_0 > 1.5$ T magnetic fields by careful adjustment of both the cryogenic and room temperature shims in a standard superconducting solenoid magnet. Lower field experiments not reported here demand the use of more sophisticated line narrowing methods that refocus magnetic field inhomogeneity while leaving chemical shifts unaffected [30]. Several water suppression strategies in full bottle wine samples can be envisioned, but the requirement for an inexpensive rapid throughput approach must be kept in mind. For example, pulsed field gradient water suppression sequences are clearly superior when small samples in standard NMR instruments are studied [31]. However, the cost in both time and equipment make these approaches unattractive for rapid throughput full bottle studies. The robust jump and return water suppression pulse sequence that performs well on $< 10\,\text{Hz} = 2.5 \times 10^{-2}$ ppm wide ^{1}H NMR lines [32] shares the same fate when one realizes that 0.25–0.5 ppm wide ^{1}H NMR lines are routinely observed in full bottle wine samples. Although inexpensive, the original soft pulse selective excitation of the methyl group region of the full bottle ^{1}H NMR spectrum takes too much time to optimize [8,9]. Both presaturation of the water peak and T_1 based filters meet with little success in full bottle wine samples as the exchange contributions to the water peak ^{1}H line width lead to inadequately edited spectra [33]. Although inexpensive and successful in water, ethyl alcohol, and acetic acid mixtures, a T_2 based filter using a spin echo proved unsuccessful in real wine samples where the acetic acid and acetaldehyde methyl group T_2 relaxation time is much shorter [34].

This paper focuses on optimizing the $1\bar{3}3\bar{1}$ phase alternated water suppression pulse sequence [35] and its application to the rapid throughput quantitation of the oxidation level of full bottles of wine. The lack of pulsed field gradients in this pulse sequence makes the method attractive from the standpoint of cost and the following sections demonstrate that the pulse sequence can be customized to yield narrow line in phase ^{1}H NMR spectra for full bottles of wine, the necessary first step towards spoilage quantitation.

2. Theory

The most promising water suppression method employed thus far in the rapid throughput study of full bottles of wine is based on the $1\bar{3}3\bar{1}$ pulse sequence shown in Fig. 1. As mentioned above, the optimal rf pulse sequence uniformly excites the methyl group proton resonances in ethyl alcohol at 1.1 ppm and acetic acid or acetaldehyde at 2.1 ppm with constant phase while removing the effects of water, here an intense peak at 4.7 ppm. It is clear that the inversion symmetry of the $1\bar{3}3\bar{1}$ pulse sequence will suppress the water signal as long as it is placed on resonance. However, it is not immediately obvious what delay time τ and delay time t_ϕ values in Fig. 1 are necessary to ensure constant phase uniform excitation at the 1.1 and 2.1 ppm methyl group proton resonances when realistic $t_{90} = 20$–$300\,\mu\text{s}$ $\pi/2$ rf pulse times are present. A reasonable

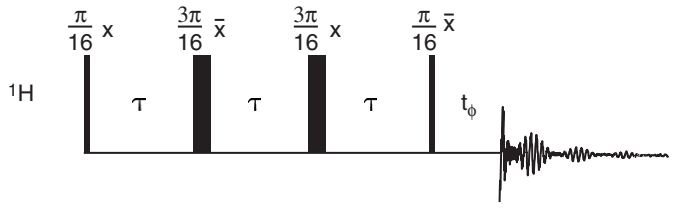

Fig. 1. The $1\bar{3}3\bar{1}$ water suppression pulse sequence used in this study showing the time delay between pulses τ and the phase delay time t_ϕ.

starting point to address these two issues is the analytical solution for the two level system transverse magnetization

$$M_+ = \sin^3\left(\frac{\delta\tau}{2}\right)e^{i\delta(3\tau/2+t_\phi)} \tag{1}$$

at the time $3\tau/2 + t_\phi$ in the limit of zero time perfect tip angle rf pulses where resonance offset effects δ are neglected during the pulse [35]. The magnetization shown in Eq. (1) when the delay time $t_\phi = 0$ yields the expected first order spectral phase encoding implicit to the $1\bar{3}3\bar{1}$ pulse sequence. Consider first the uniform excitation of the two methyl-group proton peaks at the angular frequencies δ_1 and δ_2 pertaining to the 2.1 and 1.1 ppm chemical shifts for acetic acid or acetaldehyde and ethyl alcohol when the water peak at 4.7 ppm is placed on resonance. This situation is realized with reference to Eq. (1) when $\sin^3(\delta_1\tau/2) = \sin^3(\delta_2\tau/2)$ or equivalently when $\sin(\delta_1\tau/2) = \sin(\delta_2\tau/2)$ implying that $\sin(\delta_1\tau/2) - \sin(\delta_2\tau/2) = 2\cos[(\delta_1+\delta_2)\tau/4]\sin[(\delta_1-\delta_2)\tau/4] = 0$. There are two situations when this difference is equal to zero; however, the useful root in the argument of the cosine yields the value for the delay time

$$\tau = \frac{2\pi}{\delta_1+\delta_2}(2n+1), \tag{2}$$

where n is a positive integer or zero. The delay time t_ϕ in Eq. (1) can be adjusted in a similar way to yield in phase peaks at the two target frequencies δ_1 and δ_2 when the difference in signal phase is a multiple of 2π. The delay time

$$t_\phi = \frac{2\pi m}{|\delta_1-\delta_2|} - \frac{3}{2}\tau \tag{3}$$

in terms of the positive integer m is obtained by setting the difference in phases obtained from Eq. (1) for isochromats at the δ_1 and δ_2 offset frequencies equal to $2\pi m$.

Having identified values for the delay times τ and t_ϕ that yield phase constant uniform excitation at both 2.1 and 1.1 ppm, the chemical shifts for the methyl group protons in acetic acid or acetaldehyde and ethyl alcohol respectively, the next step is to determine whether or not the delay times anticipated on the basis of a simple two level model properly excite two chemically shifted lines, even when realistic $t_{90} = 20-300\,\mu s$ $\pi/2$ rf pulse times are present and when one resonance displays scalar J couplings. To address this issue a numerical simulation that solves the Liouville von Neumann equation

$$\frac{d}{dt}\rho(t) = -i[H,\rho(t)] \tag{4}$$

in the rotating frame was performed. In this case the Hamiltonian during the time delay τ in Fig. 1 given by

$$H = \delta_1\sum_{i=1}^{3}K_{z,i} + \delta_2\sum_{i=1}^{3}I_{z,i} + \delta_3\sum_{i=1}^{2}S_{z,i} + J\sum_{i=1}^{3}\sum_{j=1}^{2}I_{z,i}S_{z,j} \tag{5}$$

reflects the secondary components in spoiled wine, namely acetic acid or acetaldehyde and ethyl alcohol. It should be clear that δ_1, δ_2, and δ_3 pertain to the frequency offsets for the methyl group protons in acetic acid or acetaldehyde, the methyl group protons in ethyl alcohol, and the methylene protons in ethyl alcohol respectively given that the water peak at 4.7 ppm is set to zero frequency in the rotating frame or equivalently on resonance. Eq. (5) also involves the spin operators appropriate for the three methyl group acetic acid protons $K_{z,i}$, the three methyl group protons in ethyl alcohol $I_{z,i}$, and the two methylene protons in ethyl alcohol $S_{z,i}$ in addition to the bilinear secular part of the scalar coupling $I_{z,i}S_{z,j}$ scaled by the $J = 6.8$ Hz coupling constant between methyl and methylene ethyl alcohol protons. During the rf pulses shown in Fig. 1, the Hamiltonian shown in Eq. (5) is augmented by the rf Hamiltonian

$$H_{rf} = \pm\omega_1\left(\sum_{i=1}^{3}K_{x,i} + \sum_{i=1}^{3}I_{x,i} + \sum_{i=1}^{2}S_{x,i}\right), \tag{6}$$

where $K_{x,i}$, $I_{x,i}$, and $S_{x,i}$ are the respective transverse angular momentum spin operators for the acetic acid or acetaldehyde methyl group protons, the ethyl alcohol methyl group protons, and the ethyl alcohol methylene protons. The ± sign multiplying ω_1 in Eq. (6) anticipates the 180° shift in rf phase prescribed by the $1\bar{3}3\bar{1}$ pulse sequence. Within the high temperature approximation, the portion of the initial thermal equilibrium density operator at the time $t = 0$ that is variant under rotations is given by

$$\rho(0) \propto f\sum_{i=1}^{3}K_{z,i} + \sum_{i=1}^{3}I_{z,i} + \sum_{i=1}^{2}S_{z,i}, \tag{7}$$

where f is a factor relating the concentration of oxidative spoilage products in wine to ethyl alcohol. This form for the density operator $\rho(0)$ is used along with H and H_{rf} in Eqs. (5) and (6) to calculate a spectrum resulting from the $1\bar{3}3\bar{1}$ pulse sequence by Fourier transformation of the expectation values of the transverse magnetization

$$M_x = \mathrm{Tr}\left\{\left(\sum_{i=1}^{3}K_{x,i} + \sum_{i=1}^{3}I_{x,i} + \sum_{i=1}^{2}S_{x,i}\right)\cdot\rho(t)\right\} \tag{8}$$

and

$$M_y = \mathrm{Tr}\left\{\left(\sum_{i=1}^{3}K_{y,i} + \sum_{i=1}^{3}I_{y,i} + \sum_{i=1}^{2}S_{y,i}\right)\cdot\rho(t)\right\}, \tag{9}$$

where $K_{y,i}$, $I_{y,i}$, and $S_{y,i}$ are operators 90° out of phase with the operators $K_{x,i}$, $I_{x,i}$, and $S_{x,i}$ and Tr{...} indicates the trace operation. The effects of both relaxation and magnetic field inhomogeneity are phenomenologically built into the simulation by multiplying the oscillating M_x and M_y signals computed in Eqs. (8) and (9) with a damped exponential function.

A final comment regarding quantitation of the amount of wine spoilage due to oxidation is necessary. In principle this estimate demands determination of the factor f in Eq. (7). This factor f is the ratio of accurately determined integrated signal intensities of the acetic acid or acetaldehyde methyl group proton peak to the ethyl alcohol methyl group proton peak. This ratio was calculated for both simulated and experimental results using a Matlab program that extracts, phases, base line corrects, and integrates using Simpson's rule the two spectral regions around 2.1 and 1.1 ppm.

3. Materials and methods

All standardized oxidation samples were prepared by mixing variable volumes of 99.7% glacial acetic acid and 200 proof ethyl alcohol with distilled water. Each of these chemical compounds was respectively obtained from E.M. Science (Gibbstown, NJ), Gold Shield Chemical Company (Hayward, CA), and an in house water distillation unit. These samples were stored in either Wilmad (Vineland, NJ) 5 mm outer diameter pyrex NMR tubes or 750 mL wine bottles both isolated from the atmosphere with parafilm tape obtained from American National Can (Menasha, WI). The standardized full bottle wine spoilage library was prepared by adding controlled volumes of acetic acid or acetaldehyde to full 750 mL bottles of Charles Shaw Merlot purchased at Trader Joe's. The small volume wine spoilage library was prepared by transferring approximately 1 mL from each of the adulterated wine bottles to separate 5 mm outer diameter pyrex NMR tubes that were later sealed with parafilm tape.

Small sample NMR measurements were accomplished at UC Davis using an Oxford Instruments (Palo Alto, CA) 9.4 T 78 mm room temperature bore superconducting solenoid magnet housing a Bruker (Billerica, MA) 78 mm shim stack and a home built 400 MHz liquid state NMR probe. Free induction signals were generated and detected with a two channel Tecmag (Houston, TX) Apollo pulse programmer equipped with a direct digital frequency source and digital data acquisition system. All small sample high field ^{1}H NMR spectra and intensity ratio data correspond to a free induction signal averaged over 16 acquisitions. Full bottle NMR data was obtained at Wine Scanner, Inc. (Morristown, NJ) using an Oxford Instruments 4.7 T 110 mm room temperature bore superconducting solenoid magnet and a custom built single channel Tecmag pulse programmer that controls a low bandwidth 200 MHz direct digital frequency source and a digital data acquisition system. The full bottle NMR spectrometer was customized with a homebuilt shim stack, probe head, and sample changer. The eight channel shim stack has three in house wound longitudinal shims (z^1, z^2, and z^3) surrounding five flexible pc board mounted tesseral shims (x, y, xz, yz, and xy) salvaged from a Bruker 78 mm shim stack. The NMR probe head has a modified Alderman–Grant resonator [36] tuned to 200 MHz and mounted on a 1.5 in Teflon funnel that doubles as a coil form and a sample holder that supports the neck of an inverted wine bottle. Finally, the inverted wine bottle is lowered into the NMR probe head from the top of the magnet cryostat with a 40 in high home built sample changer fastened to the top cryostat vacuum flange. Vertical motion of the sample changer is accomplished with a 40 in long drive screw controlled by a Lorring and Associates (Dublin, CA) integrated stepper motor. All full bottle low field ^{1}H NMR spectra and intensity ratio data correspond to a free induction signal averaged over eight acquisitions.

4. Results and discussion

It is important to consider optimum τ and t_ϕ delay time values for both high field $B_0 = 9.4$ T, high resolution, small sample and lower field $B_0 = 4.7$ T, comparatively lower resolution, full bottle studies of wine oxidation as sensory level contaminant concentrations are on the order of 750 mg/L or equivalently a chemically shifted proton peak at 2.1 ppm with an intensity roughly 0.015% of the water peak. Eqs. (2) and (3) are extremely useful in determining appropriate choices of delay time τ and t_ϕ values in both the small sample and full bottle limit where magnetic field inhomogeneity effects are drastically different. In the case of small samples contained in standard 5 mm NMR tubes, narrow Lorentzian shaped peaks are routinely observed by adjusting the room temperature shims. On the other hand, NMR studies of full intact wine bottles often yield very broad irregularly shaped peaks due to susceptibility artifacts established by paramagnetic impurities in the glass bottle, trace magnetism in the metal foil, and finite sample volume as the rf coil encloses the neck of the wine bottle immediately next to the cork [8,9]. Even though the cryogenic and room temperature shims can be adjusted to compensate for these effects, bottle-to-bottle variations in overall sample shape, in the metal seal and glass composition, and in the size of the cork and its placement in the wine bottle, non-Lorentzian two component peak shapes still result making the identification of contaminants in full wine bottles difficult. A solution to this line width problem couples this observation with the simple fact that there is an abundance of sample and with an earlier experiment in the proton NMR spectra of solids [37]. Here a measurement time delay, the time t_ϕ shown in Fig. 1, is used to eliminate the fast decaying components of the transient NMR signal by digitizing just the long time tail of the free induction signal. The beauty of the pulse sequence shown in Fig. 1 is that as long as the delay times τ and t_ϕ are chosen appropriately with respect to Eqs. (2) and (3),

narrow line, water suppressed, in phase full bottle NMR spectra can be obtained. Delay time τ and t_ϕ values calculated from Eqs. (2) and (3) are shown in Table 1 for application to both $B_0 = 9.4\,\mathrm{T}$ small sample studies where t_ϕ is only used to establish in phase methyl group proton signals and $B_0 = 4.7\,\mathrm{T}$ full bottle experiments where long t_ϕ times are required for both phase correction and artificial line narrowing.

The plots shown in Figs. 2 and 3 compare the effects of the delay time τ and t_ϕ values shown in Table 1 to numerical simulations. The overall excitation bandwidth of the $1\bar{3}3\bar{1}$ pulse sequence within the two level system zero time rf pulse limit of $|\sin^3(\delta\tau/2)|$ in Eq. (1) is shown in Figs. 2(a) and 3(a) for the high field small sample delay time $\tau = 380\,\mu\mathrm{s}$ and the lower field full bottle sample delay time $\tau = 720\,\mu\mathrm{s}$ respectively. A comparison of these excitation profiles to the results of an eight spin simulation with an artificially inflated $f = 1/6$ value and with the delay time $t_\phi = 0$ and the delay time t_{90} values shown in Table 1 is provided in Figs. 2(b) and 3(b) for high and low field respectively. Although both of the peaks at 1.1 and 2.1 ppm are uniformly excited in comparison to Figs. 2(a) and 3(a), they are not in phase since the delay time $t_\phi = 0$. Application of the delay time t_ϕ values calculated from Eq. (3) and listed in Table 1 generates the in phase uniformly excited spectra shown in Figs. 2(c) and 3(c) at high and low field respectively. As expected, the ratio of the integrals of the peak at 2.1 ppm to the peak at 1.1 ppm recovers the fraction $f = 1/6$ for both the high field and low field simulations shown in Figs. 2(c) and 3(c).

The spectra shown in Fig. 4 demonstrate the predictions of these simulations applied to a prepared small sample in Fig. 4(a) and a full bottle sample in Fig. 4(b) containing 0.3% (v/v) acetic acid, 12.0% (v/v) ethyl alcohol, and 87.7% (v/v) water. Careful integration of the peaks at 2.1 and 1.1 ppm yields values that can be used to calculate the ratio of acetic acid to ethyl alcohol in the prepared samples and thus an estimate of artificially created oxidation. The 0.020 ± 0.002 and 0.025 ± 0.004 ratios obtained from five separate measurements like those shown in Fig. 4 for small samples in (a) and full bottles in (b) compare well with the 0.023 concentration ratio anticipated on the basis of sample preparation. The factor of 0.91 and 1.1 difference between the measured average and expected concentration ratios is used as an instrumental correction factor for the quantitation of oxidative spoilage in real wine samples.

The bar graph shown in Fig. 5 compares estimates of the ratios of acetic acid to ethyl alcohol concentrations in wine adulterated with acetic acid determined by high field NMR applied to small samples (gray bar with black circle) and lower field NMR applied to full bottles (gray bar with black diamond) to the actually prepared ratio (black bar). Each point corresponds to the average of five separate measurements and the error bars accompanying these averages sets the 95% confidence limit. The bottom and left

Table 1
Comparison of low and high field τ and t_ϕ values

B_0	9.4 T	4.7 T
δ_1	7.10×10^3 rad/s	3.55×10^3 rad/s
δ_2	9.38×10^3 rad/s	4.69×10^3 rad/s
n	0	0
m	2	4
t_{90}	30 μs	100 μs
τ	380 μs	762 μs
t_ϕ	4.9 ms	20.9 ms

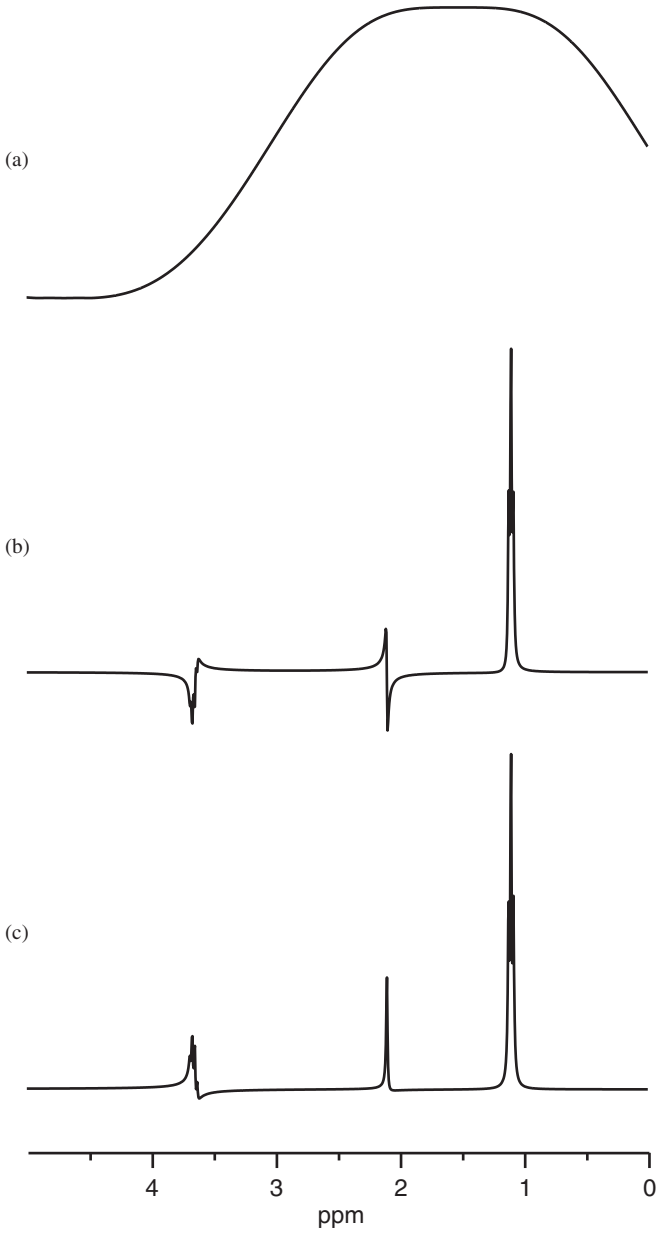

Fig. 2. Simulations showing the effect of the $1\bar{3}3\bar{1}$ pulse sequence at $B_0 = 9.4\,\mathrm{T}$ on an ethyl alcohol acetic acid mixture. The excitation pattern shown in (a) and the spectra shown in (b) and (c) correspond to $\tau = 380\,\mu\mathrm{s}$ pulse delay time and $t_{90} = 30\,\mu\mathrm{s}$ $\pi/2$ rf pulse time values and a phase delay time $t_\phi = 0$ in (b) and $t_\phi = 4.9\,\mathrm{ms}$ in (c).

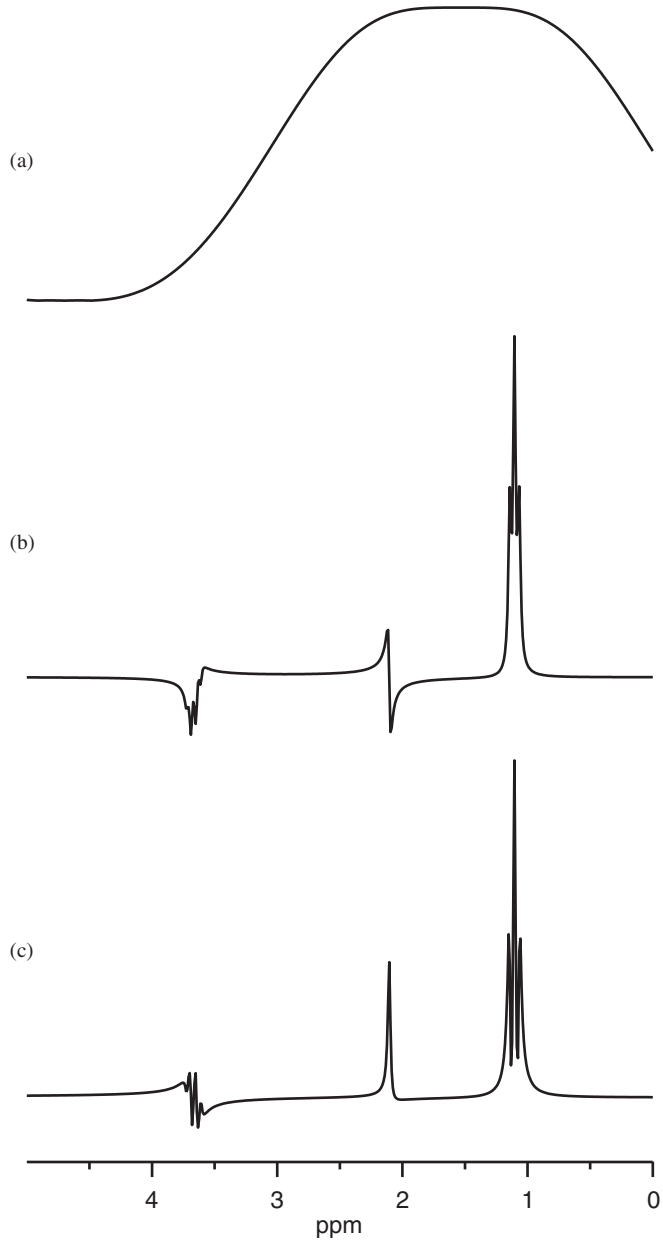

Fig. 3. Simulations showing the effect of the $1\bar{3}3\bar{1}$ pulse sequence at $B_0 = 4.9\,\mathrm{T}$ on an ethyl alcohol acetic acid mixture. The excitation pattern shown in (a) and the spectra shown in (b) and (c) correspond to $\tau = 762\,\mu\mathrm{s}$ pulse delay time and $t_{90} = 100\,\mu\mathrm{s}$ $\pi/2$ rf pulse time values and a phase delay time $t_\phi = 0$ in (b) and $t_\phi = 20.9\,\mathrm{ms}$ in (c).

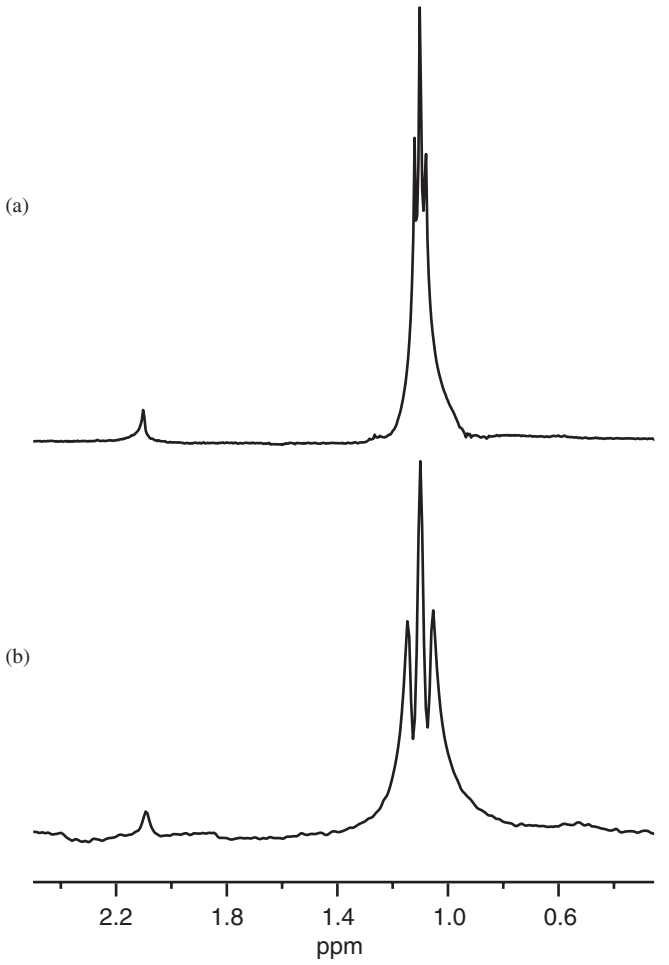

Fig. 4. Small sample high field in (a) and full bottle low field in (b) $1\bar{3}3\bar{1}$ suppressed ^{1}H NMR spectra for a 0.3% (v/v) acetic acid sample. The peak at 1.1 ppm is the characteristic triplet for the methyl group in ethyl alcohol while the resonance at 2.1 ppm corresponds to the methyl group singlet in acetic acid.

axes pertain to integrated peak ratio estimates while knowledge of the 12.5% (v/v) ethyl alcohol concentration in these wines is used to calculate the actual concentration of acetic acid [9], defined here by the top and right axes. It is clear from Fig. 5 that the small sample and full bottle estimates of the concentration ratio of acetic acid to ethyl alcohol are consistent with each other and the prepared concentration within the random error indicated by the vertical 95% confidence limit error bars for the three highest prepared concentrations. This agreement is not as strong for the two lower prepared acetic acid concentrations shown in Fig. 5 due to either inadequate signal to noise for the 2.1 ppm peak reflecting the limited number of acquisitions used to maintain the rapid throughput nature of the experiment, an error in sample preparation, or the presence of a background amount of either acetic acid or acetaldehyde in the native wine. The effect of a limited number of signal acquisitions is observed for all of the measured data points shown in Fig. 5 as there is greater error noticed in each full bottle data point where only 8 signals at 4.7 T were accumulated versus each small sample data point where 16 signals at 9.4 T were averaged. Indeed it has been shown [8] that the accumulation of a greater number of signals, a process taking much less time than room temperature shimming, will relieve any discrepancy between the small sample and the full wine bottle standards. The possibility of an error in sample preparation is most likely not the origin of the deviation shown for the lowest concentration in Fig. 5 as NMR based measurements for standardized wine samples prepared from inexpensive wines like the Charles Shaw Merlot used here are routinely higher than anticipated. The reason for

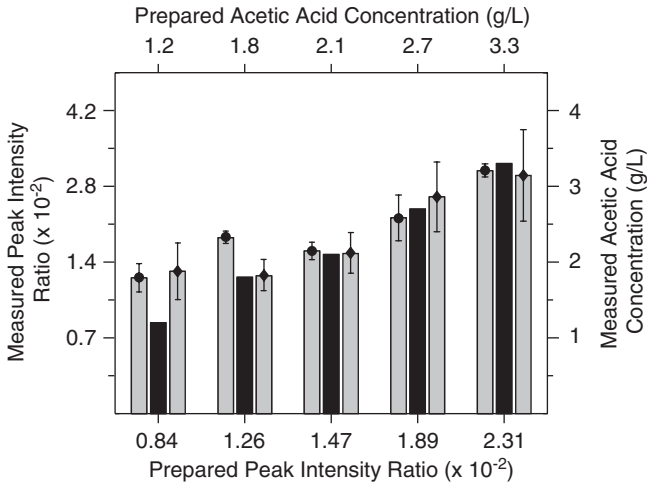

Fig. 5. Bar graph comparing small sample high field (gray bar with black circle), full bottle low field (gray bar with black diamond), and actual (black bar) measurements of acetic acid concentration in adulterated wine samples. The lower abscissa and left ordinate correspond to integrated NMR peak intensity ratios while the upper abscissa and right ordinate use the experimental peak intensity ratio with the known 12.5% (v/v) amount of ethyl alcohol in the wine to determine the concentration of acetic acid. The error bars set the 95% confidence limit.

this artificially inflated NMR based oxidation level estimate is revealed in the NMR spectra where oxidation products are observed for the native wine samples used to prepare the standardized library. In fact, the NMR based methods accurately measure the total amount of oxidation products in the wine and it is only at the lower prepared concentrations that the effects of background quantities are revealed.

The power of this method of full bottle wine characterization is two fold. On one hand it permits an estimate of wine spoilage as shown in Fig. 6 where a comparison of an unopened full bottle of the 1914 vintage of Clos de Tart in (a) to an unopened bottle of the 1888 vintage of Chateau Latour in (b) is provided. The lack of any clear peak in comparison to noise at 2.1 ppm in (b) suggests limited oxidative spoilage of the 26 year older Latour in comparison to the Clos de Tart. The observation in (b) for the 1888 Latour averaging just 8 signals is consistent with the spectrum accumulated with increased signal averaging. Integration of the peaks at 2.1 and 1.1 ppm shown in Fig. 6(a) can be used to estimate the 0.012 ± 0.003 ratio of acetic acid or acetaldehyde to ethyl alcohol—a prediction that renders the presumably valuable wine worthless. Combining this ratio with the quoted 12% ethyl alcohol content in the Clos de Tart or equivalently a measurement of the ethyl alcohol content from integrals of the peak at 1.1 ppm to the water peak at 4.7 ppm obtained from the usual one dimensional proton NMR spectrum following one rf pulse [9] yields an acetic acid or acetaldehyde concentration of $1.7 \pm .2$ g/L. It is important to note that the ^{1}H NMR spectrum shown in Fig. 6(a) cannot distinguish between acetic acid or acetaldehyde contaminants since the difference in chemical shifts of the

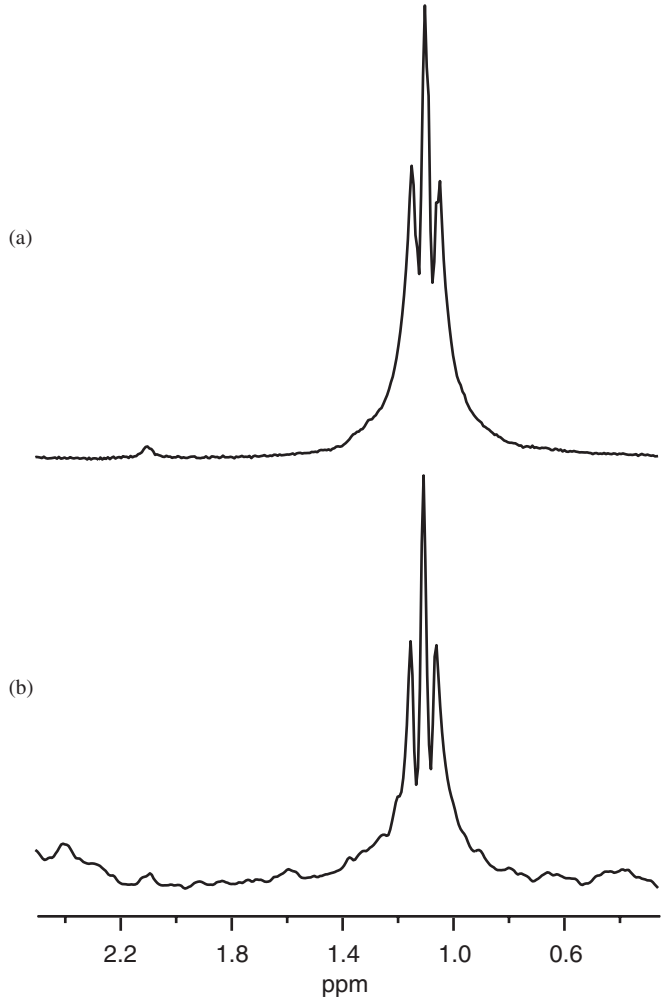

Fig. 6. Full bottle low field $1\bar{3}3\bar{1}$ water suppressed ^{1}H NMR spectra for the 1914 Clos de Tart in (a) and the 1888 Chateau Latour in (b).

methyl group proton peak for acetic acid and acetaldehyde is below the measurement resolution. The lack of any aldehyde peak at 9.8 ppm in the Clos de Tart (spectrum not shown) suggests that the contaminant is due to acetic acid. A second advantage of the carefully designed $1\bar{3}3\bar{1}$ pulse sequence with the time delay t_ϕ applied to full wine bottle studies is that rapid throughput is realized. The time delay t_ϕ substantially relaxes the need for time-consuming magnetic field shimming. In fact the 27 full bottle measurements reported above were accomplished in a few hours, a clear cost and time benefit in comparison to other more expensive methods requiring pulsed field gradients or time consuming frequency selective excitation or saturation where careful pulse calibration is required.

5. Conclusion

The $1\bar{3}3\bar{1}$ water suppression pulse sequence customized with the delay time t_ϕ is used to develop a rapid throughput method to study oxidation products in full bottles of wine. This pulse sequence addresses both the demand for narrow NMR lines without massive time expense on room

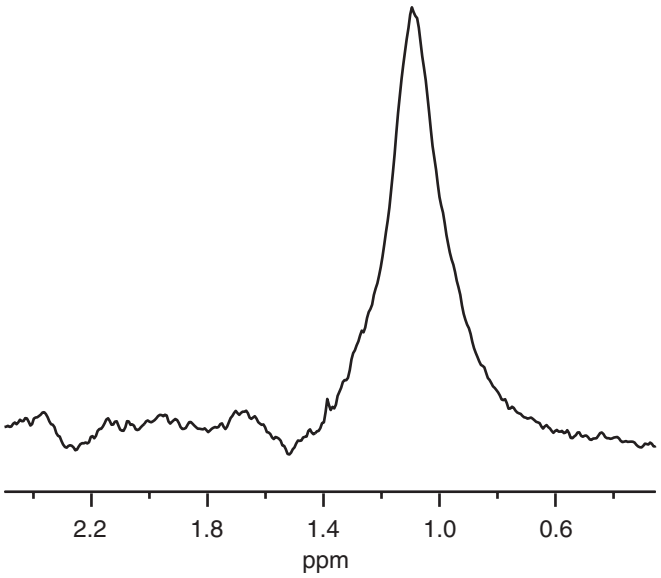

Fig. 7. Full bottle low field $1\bar{3}3\bar{1}$ water suppressed ^{1}H NMR spectrum for the 1970 Chateau Latour. The lack of any methyl group triplet resolution reflects the limited time spent on room temperature shimming.

temperature shimming and on spectrometer calibration. The first goal is realized by choosing long delay time t_{ϕ} values while the second is automatically provided once the probe is tuned, the $\pi/2$ rf pulse time t_{90} is identified, and the water peak at 4.7 ppm is placed on resonance. Accomplishing these minor requirements insures that full bottles of wine can be screened for oxidation products in less than 10 min/bottle, a necessary requirement given the estimated nine million bottles of collectible wine available for investigation.

In closing, it should be mentioned that exotic applications of NMR spectroscopy like the one discussed here are a recurring theme in the career of Alex Pines. His vision and creativity have pushed NMR spectroscopy from its roots in physics to materials science, biochemistry, medicine, aerospace, engineering, etc. both directly and indirectly by mentoring undergraduate students, graduate students, and post-docs and by collaborating with scientists from around the world. It is indeed an honor to provide this manuscript to an issue of Solid State NMR commemorating Alex's 60th birthday as his direct impact on our careers cannot be stated in words. As a token of our appreciation of Alex's contributions to the field of NMR, we have shipped him a bottle of 1970 Chateau Latour, a fine Bordeaux that is pristine judging from the lack of any peak at 2.1 ppm in Fig. 7.

Acknowledgment

A useful email discussion with Ralph Hurd regarding full bottle NMR and the assistance provided by Doug Crane with all full bottle NMR experiments is gratefully acknowledged. MPA is a David and Lucile Packard and Alfred P. Sloan Foundation Fellow.

References

[1] D.M. Grant, R.K. Harris (Eds.), Encyclopedia of Nuclear Magnetic Resonance, Wiley, Chichester, UK, 2002.
[2] R.R. Ernst, G. Bodenhausen, A. Wokaun, Principles of Nuclear Magnetic Resonance in One and Two Dimensions, Oxford University Press, New York, 1987.
[3] P.C. Lauterbur, Nature 242 (1973) 190–191.
[4] P. Mansfield, P.K. Grannell, J. Phys. C 6 (1973) L422–L426.
[5] C.T.W. Moonen, P.A. Bandettini (Eds.), Functional MRI, Springer, New York, 1999.
[6] P.T. Callaghan, Principles of Nuclear Magnetic Resonance Microscopy, Oxford University Press, New York, NY, 1991.
[7] P.T. Callaghan, in: D.M. Grant, R.K. Harris (Eds.), Encyclopedia of Nuclear Magnetic Resonance, Wiley, Chichester, UK, 2002, pp. 737–750.
[8] A.J. Weekley, P. Bruins, M.P. Augustine, Am. J. Enol. Vitic. 53 (2002) 318–321.
[9] A.J. Weekley, P. Bruins, M. Sisto, M.P. Augustine, J. Magn. Reson. 161 (2003) 91–98.
[10] R. Hurd, 24th Experimental NMR Conference, Pacific Grove, CA, 1983.
[11] W.I. Jung, O.Lutz, K. Mueller, M. Pfeffer, K. Kuper, Proceedings of the 8th Annual Meeting Soc. Magazine. Res. Med., Amsterdam, Netherlands, 1989, p. 637.
[12] A. Rapp, A. Markowetz, Chem. Unserer Zeit 3 (1993) 149–155.
[13] A. Rapp, A. Markowetz, M. Spraul, E. Humpfer, Dtsch. Lebensm. Rundsch. 83 (1987) 375–378.
[14] G.J. Martin, M.L. Martin, F. Mabon, M. Michon, Anal. Chem. 54 (1982) 2380–2382.
[15] M.P. Day, B. Zhang, G.J. Martin, J. Sci. Food Agric. 67 (1995) 113–123.
[16] C. Guillou, F. Reniero, Phys. World 11 (1998) 22–23.
[17] O. Lutz, E. Humpfer, M. Spraul, Naturwissenschaften 18 (1991) 67–69.
[18] I. Kosir, M. Kocjancic, J. Kidric Analusis. 26 (1998) 97–101.
[19] I. Kosir, J. Kidric, Anal. Chim. Acta 458 (2002) 77–84.
[20] C. Saucier, I. Pianet, M. Laguerre, Y. Glories, J. Chim. Phys. 95 (1998) 357–365.
[21] E.J. Waters, Z. Teng, K.F. Pocock, G.P. Jones, P. Clarke, P.J. Williams, J. Agricult. Food Chem. 42 (1994) 1761–1766.
[22] K. Matsushita, M. Nishina, T. Asakura, S. Kamei, M. Suzuki, K. Yabe, Phys. Chem. Phys. Med. NMR 32 (2000) 13–19.
[23] R. Baltenweck-Guyot, J. Trendel, P. Albrecht, A. Schaeffer, J. Agric. Food Chem. 48 (2000) 6178–6182.
[24] G.S. Drysdale, G.H. Fleet, Am. J. Enol. Vitic. 39 (1988) 143–154.
[25] P. Ribereau-Gayon, Am. J. Enol. Vitic. 36 (1985) 1–10.
[26] B.W. Zoecklein, K.C. Fugelsang, B.H. Gump, F.S. Nury, Wine Analysis and Production, Aspen Publishers, Gaithersburg, MD, 1995.
[27] E. Fredrikson, Wine Consultant, Gomberg, Germany, personal communication.
[28] J. Laube, Wine Spectator, March 31, 2005, pp. 44–53.
[29] C. Silva Pereira, J.J. Figueiredo Marques, M.V. San Romao, Crit. Rev. Microbiol. 26 (2000) 147–162.
[30] C.A. Meriles, D. Sakellariou, H. Heise, A.J. Moule, A. Pines, Science 293 (2001) 82–85.
[31] T. Hwang, A.J. Shaka, J. Magn. Reson. A 112 (1995) 275–279.
[32] P. Plateau, M. Guereon, J. Am Chem. Soc. 104 (1982) 7310–7311.
[33] D.N. Sobieski, M.P. Augustine, Proceedings of 45th ENC, Pacific Grove, CA, 2004, p. 71.
[34] D.N. Sobieski, M. P. Augustine, Proceedings of 229th ACS, San Diego, CA, 2005.
[35] P.J. Hore, J. Magn. Reson. 55 (1983) 283–300.
[36] D.W. Alderman, D.M. Grant, J. Magn. Reson. 36 (1979) 447–451.
[37] S. Ding, C.A. McDowell, J. Magn. Reson. A 111 (1994) 212–214.